IEEE Access
Multidisciplinary | Rapid Review | Open Access Journal

Received February 19, 2019, accepted March 1, 2019, date of publication March 5, 2019, date of current version May 22, 2019.

Digital Object Identifier 10.1109/ACCESS.2019.2903149

A Wideband-to-Narrowband Rectangular Dielectric Resonator Antenna Integrated With Tunable Bandpass Filter

BEI-JIA LIU[1], JING-HUI QIU[1], SHENG-CHANG LAN[1], AND GUO-QIANG LI[2]
[1]Department of Microwave Engineering, Harbin Institute of Technology, Harbin 150001, China
[2]Department of Automatic Image Recognition, Harbin Kejia General Mechanical and Electrical Company, Harbin 150060, China

Corresponding author: Bei-Jia Liu (liubeijia@hit.edu.cn)

This work was supported in part by the National Natural Science Foundation of China under Grant U1633202 and Grant 61731007.

ABSTRACT A compact, frequency-reconfigurable dielectric resonator antenna (DRA) with wideband and continuously tunable narrowband states is presented. It is intended for the application scenario in the cognitive radio system. The wideband state is the sensing state and operationally covers 3.82–8.94 GHz. The narrowband states are intended to cover communications within the 5.14–5.98 GHz range, which completely covers the WLAN frequency bands. Three p-i-n diodes are employed to switch between wide and some narrowband operational states by selecting the corresponding path. A varactor diode is used to shift the operational frequencies continuously among the narrowband states. The proposed DRA consists of a rectangular dielectric resonator excited by microstrip feedline with a reconfigurable filter; it has a compact dimension: $0.31\lambda_L \times 0.41\lambda_L \times 0.06\lambda_L$, where the wavelength λ_L corresponds to the lower bound of its operating frequencies. The measured reflection coefficients, far-field radiation patterns, and realized gains for both operation states are in good consistent with their simulated values.

INDEX TERMS Cognitive radio, dielectric resonator antenna, frequency reconfiguration, filter antenna, continuously tuning.

I. INTRODUCTION

To efficiently utilize the limited spectrum resources, cognitive radio (CR) system based on smart and dynamic spectrum access is proposed. A CR-based system not only monitors the spectrum hole in the finite frequency range, but also adjusts its transmission and receiving properties to work within the occupied frequency bands. The system requires a wideband antenna sensing the under-utilized or unoccupied spectrum ranges, and multiple narrow bands within the whole range are desirable as communication antenna for certain application scenarios [1], [2]. Antenna design for CR applications has been a research hotspot for several years.

Frequency reconfigurable antenna is promising, efficient and compact method for supporting CR system for scanning and communicating, compared with the configurations using separate antennas for meeting the requirement for wideband and narrowband with size increment [3], [4]. On the one hand, reconfigurable antennas with continuously tunable narrowband have been proposed, including monopole, filtenna, grid-slotted patch and so on [5]–[7]. On the other hand, wideband and fixed narrowband(s) are incorporated into one reconfigurable antenna designs controlled by p-i-n diodes or GaAs field effect transistors are extensively investigated for monopole and slot antenna in [8]–[11]. Furthermore, several frequency reconfigurable antennas with wideband and continuously tunable characteristics are reported, which are very attractive for CR applications. They are achieved by coupling reconfigurable resonators to the feed or multiple ports, all implementing by varactor diodes for continuously capacitances at proper positions of narrowband states [12]–[16].

Dielectric resonator antenna (DRA) has been extensively studied because of its extraordinary advantages of light weight, compact size, flexible design freedom, high radiation efficiency, low loss and ease to excite. It is supposed to a promising solution for ultrwideband (UWB) system [17], [18]. Moreover, there have been some frequency

The associate editor coordinating the review of this manuscript and approving it for publication was Hayder Al-Hraishawi.

TABLE 1. Final dimensions of the proposed antenna.

Parameters	a	b	c	h	g	d
Value(mm)	12	15	4	1	0.5	3
Parameters	w1	l1	w	l	x	ε_{dr}
Value(mm)	5.4	3	2	22.5	24	9.9
Parameters	x1	x2	y1	y2	y3	ε_{sr}
Value(mm)	2.4	5.2	16	16	2.4	4.4

reconfigurable DRAs reported newly, using several parasitic strips and slots, obtaining two bandwidths with two ports, changing the height of colloidal dispersion, selecting different feeding positions and varying the differential feed by varactors [19]–[28]. A frequency-tunable differentially fed DRA is investigated in [19], whose tunable resonant frequency range is about from 2.6 GHz to 2.76 GHz by chip varactors. Wang presented a integrated UWB/ narrowband DRA for cognitive radio with two ports connecting to a bevel-shaped patch and a strip seperately in [22]. Unfortunately, there is hardly any the type of frequency reconfigurable DRA with wideband state and continuously narrowband state simultaneously published in the periodical literatures.

In this paper, a wideband-to-narrowband rectangular DRA with integrated tunable bandpass filter is proposed. Section II describes the proposed antenna geometry, frequency reconfiguration mechanism and performance study including wideband DRA and tunable filter. The prototype of antenna, test and some key results and analysis are provided in Section III, followed by a concise summary and brief conclusion and prospect from the presented work in Section IV.

II. ANTENNA DESIGN

A. ANTENNA GEOMETRY

Fig.1 depicts the proposed frequency-reconfigurable DRA configuration, which consists of rectangular DR excited by offset microstrip feed network, defected ground plane and diodes. It printed on a 1 mm thick FR4 substrate with the dielectric constant of 4.4 and loss tangent of 0.02. The top layer of the substrate is composed by two paths: an uniform impedance 50 Ω microstrip line with a p-i-n diode, an O-shaped resonant structure with a varactor diode shorted to ground plane by metallic via and two p-i-n diodes between them as depicted in Fig. 1(b). A partial ground plane with a 5.2 mm×2.4 mm rectangular slot is printed on the bottom layer of the substrate as shown in Fig. 1(d). The rectangular DR has a dielectric constant of 9.9, a length of a, a width of b and a height of c. For a given dielectric constant, the aspect ratios of a/c and b/c determine resonant frequency and bandwidth of DRA. The dimensions and locations of feedline and ground plane affect the operating modes and frequency bandwidth. It is necessary to adjust some parameters of the antenna for the desired band responses. The detailed dimensions of the proposed antenna are listed in Table 1.

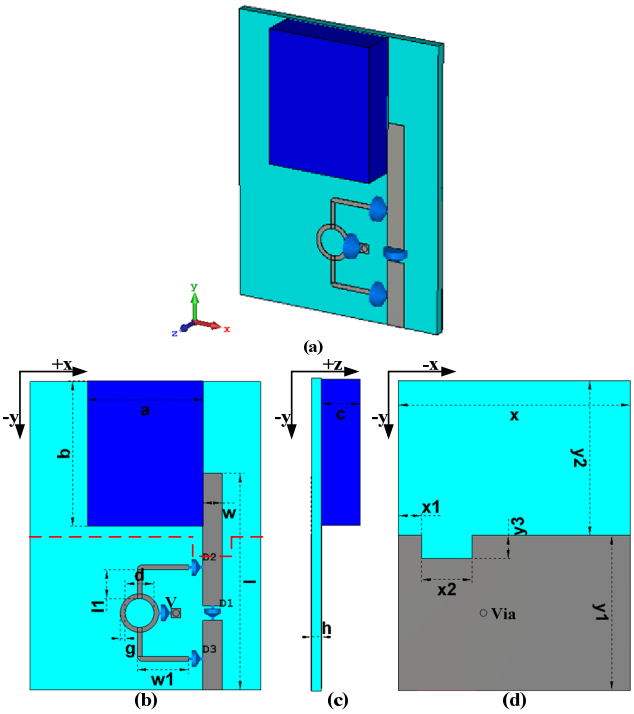

FIGURE 1. Geometry of the proposed frequency-reconfigurable rectangular DRA: (a) perspective view, (b) top view, (c) side view and (d) back view.

TABLE 2. Operation states of the proposed antenna.

State	D1	D2	D3	Performance
I	ON	OFF	OFF	Wideband
II	OFF	ON	ON	Narrow band

B. FREQUENCY RECONFIGURABLE MECHANISM

For achieving the wideband-to-narrowband tunable DRA, a new design concept of wideband DRA integrated with tunable bandpass filter is proposed. The wideband DRA is based on rectangular DR excited by offset microstrip feedline with a defected ground plane. An O-shaped uniform impedance resonator with a varactor diode is used as the filter for realizing continuously tunable narrowband characteristics. The feed network for the proposed DRA combines the microstrip line path with the filter path by p-i-n diodes, and it can select different RF path by activating corresponding p-i-n diodes. As a result, the operation frequencies of the proposed DRA are based on the reconfigurable feed network and transform agilely by dc biased voltages between wideband state and tunable narrow band state. The two reconfigurable states of the proposed DRA along with on-off states of different p-i-n diodes are presented Table 2.

C. PERFORMANCE STUDY

The proposed DRA is numerically simulated, modeled and optimized by CST@ electromagnetic simulator which utilizes the finite integration technique in this paper. A series of parametric studies was conducted for understanding

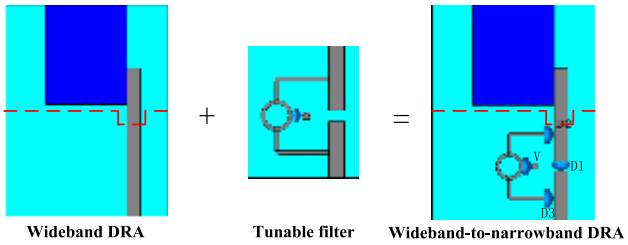

FIGURE 2. Schematic diagrams of proposed antenna.

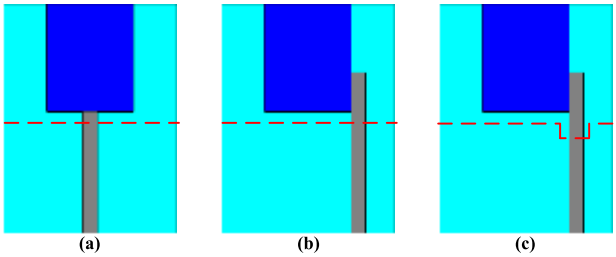

FIGURE 3. Evolution process of band enhancement DRA: (a) Antenna I, (b) Antenna II and (c) Antenna III.

how the detail dimensions affect the performance of the proposed DRA. Throughout the performance study, ideal switches with none for off state and metal bridges for on state instead of p-i-n diodes are used for choosing RF paths. Some key performances in the design process are demonstrated as follows.

1) WIDEBAND STATE

Three DRA prototypes are designed for illustrating the evolution process of band enhancement rectangular DRA based on the multiple modes characteristics and impedance matching techniques depicted in Fig. 3. Antenna I, a rectangular DRA fed by central microstrip coupling is proposed for wideband performance based on the fusion of fundamental mode and higher-order mode(s), which is estimated initial dimensions according dielectric waveguide model. For Antenna II, unsymmetrical feedline to the location DR is introducing for the purpose of exciting more modes. On the basis, defected ground plane with the rectangular notch at the center of feedline is incorporated for better impedance matching.

Simulated input reflection coefficients for the three antennas are demonstrated in Fig. 4. Antenna I works simultaneously at two excited resonant modes of 4.39 GHz and 5.03 GHz with a merged −10 dB impedance bandwidth of 2.89 GHz. Antenna II with offset microstrip feedline excites multiple modes, and presents a trend of expanding the bandwidth of high frequency. However, the input reflection energy suffers a dramatic increase, weakening the intensity of resonances. Because of the introduction of rectangular notch in ground plate, Antenna III operates at broaden impedance bandwidth of 5.12 GHz ranging from 3.82 GHz to 8.94 GHz for the better impedance matching. Moreover, the same defected ground structure design for central fed

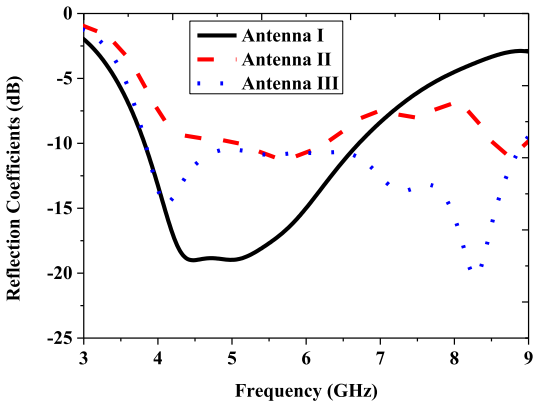

FIGURE 4. Simulated input reflection coefficients of the three antennas.

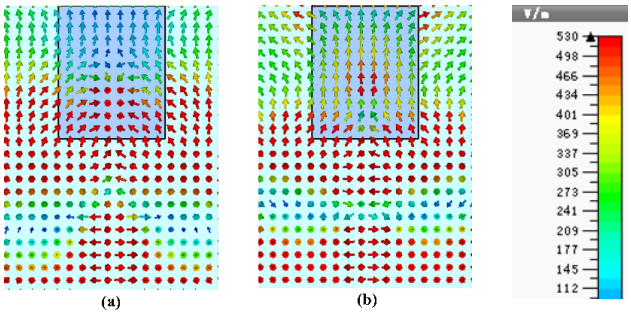

FIGURE 5. Electric field distributions in top views of Antenna I: (a) 4.39 GHz and (b) 5.03 GHz.

DRA in Fig. 3(a) was also investigated, and no obvious band enhancement was obtained. It can be concluded that the band enhancement for the proposed rectangular DRA is the result of joint effect of offset excitation and partial ground plane with defected structure at proper position.

Fig.5 demonstrates the electric field distributions ranging from 0 V/m to 530 V/m in top views of Antenna I at two resonant frequencies with central feedline. The symmetrical excitation results in symmetrical field distributions and makes the amount of energy to build along with the feedline direction for both the two operate modes. In addition, the field distributions are different between 4.39 GHz and 5.03 GHz and it can be observed that the electric fields concentrate on the half bottom near the microstrip feedline for the lower frequency, while they transforms upward along the y-axis direction with maximum electric field area located at the center of the rectangular DR for the higher frequency.

Simulated electric field distributions ranging from 0 V/m to 770 V/m in top views of Antenna III at four resonant frequencies of 4.12 GHz, 5.45 GHz, 7.29 GHz and 8.28 GHz are shown in Fig.6, which correspond to the fundamental mode and three higher-order modes. Thereinto, a strong resonance of quasi TE_{12^δ} mode at 8.28 GHz is excited.

2) TUNABLE NARROWBAND STATE

The tunable narrowband state is created by choosing the RF path of adjustable bandpass filter incorporated into the

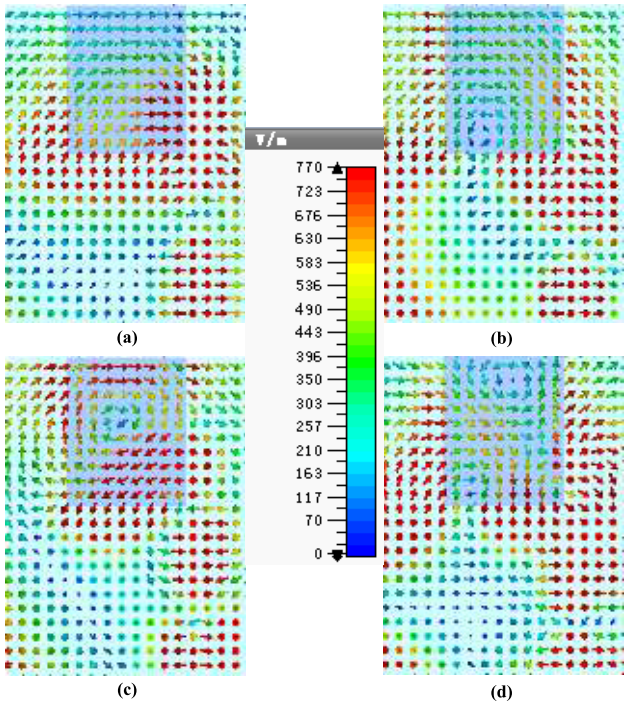

FIGURE 6. Electric field distributions in top views of Antenna III: (a) 4.12 GHz, (b) 5.45 GHz, (c) 7.29 GHz and (d) 8.28 GHz.

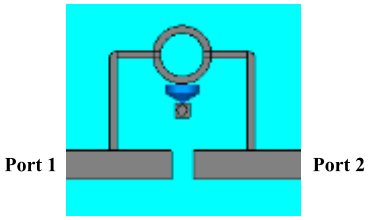

FIGURE 7. Geometry of the proposed tunable O-shaped bandpass filter.

feedline with ideal on-and-off switches as depicted in Fig. 7. The frequency tunable range depends on the dimension including the diameter of the circular ring and the width of the stip for the proposed resonant structure. In addition, the varactor diode, which provides a continuously varying capacitance for changing the even-mode resonant frequency of the proposed symmetrical O-shaped filter, affects the adjustable range to some extent. The varactor diode of SMV 1247-079LF produced by Skyworks is use for the proposed filter. Its simplified equivalent circuit model for the simulation is described in Fig. 8, according to the published datasheet. The equivalent circuit model is composed of a junction capacitance C_J ranging from 0.64 pF to 8.86 pF operated respectively by a reverse bias voltage ranging from 8 V to 0 V, a series resistance $R_S = 0.5\ \Omega$, a resistance inductance $L_S = 0.7$ nH and a parasitic capacitance $C_p = 0.05$ pF. Some relationships between capacitance and reverse voltage of SMV1247-079LF are indicated in Tab. 3.

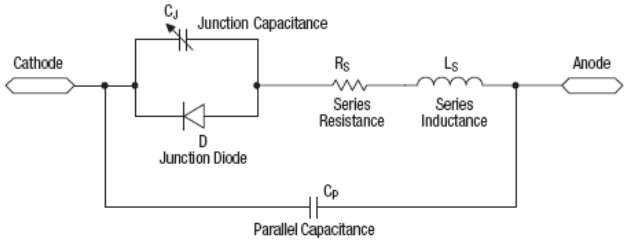

FIGURE 8. Simplified equivalent circuit model of varactor diode.

TABLE 3. Capacitance vs reverse voltage of SMV1247-079LF.

V_R [V]	0	0.5	1	1.5	2	2.5	3	3.5	4
C_T [pF]	8.86	6.17	4.37	2.96	1.88	1.22	0.95	0.83	0.77

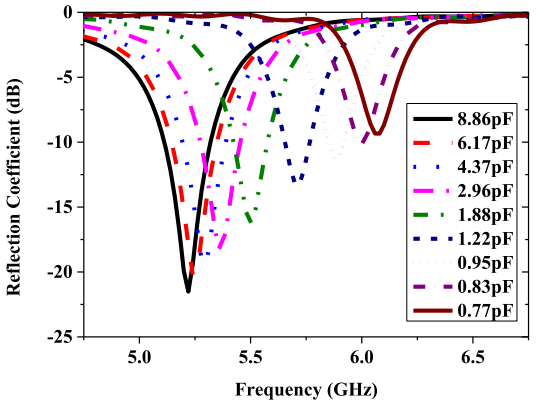

FIGURE 9. Simulated reflection coefficients of the tunable bandpass filter.

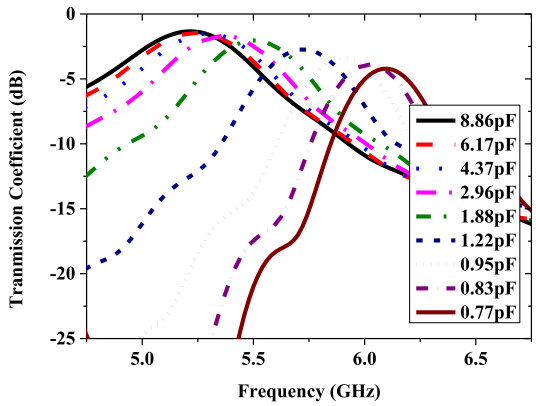

FIGURE 10. Simulated transmission coefficients of the tunable bandpass filter.

The simulated reflection coefficients of the tunable bandpass filter are shown in Fig. 9, which manifests that the tunable resonant frequencies range from 5.22 GHz to 6.07 GHz with the junction capacitances ranging from 8.86 pF to 0.77 pF and the resonant depths weaken with the increase of resonant frequency. Fig. 10 demonstrates the simulated transmission coefficients of the tunable bandpass filter.

III. RESULTS AND ANALYSIS

To verify the design feasibility for reconfigurable rectangular DRA with wide-to-narrowband characteristic, a prototype of

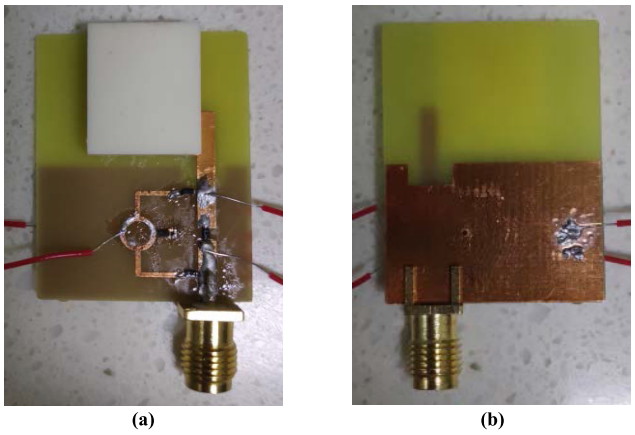

FIGURE 11. Prototype of the proposed frequency-reconfigurable rectangular DRA.

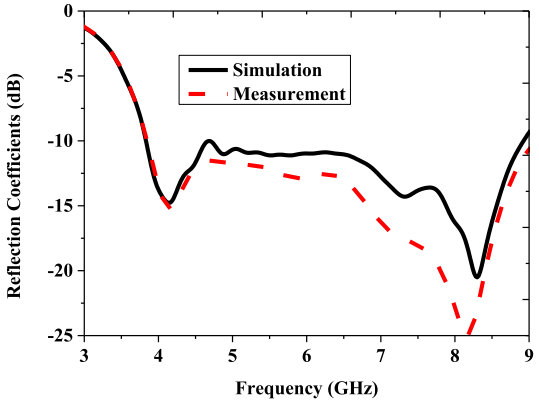

FIGURE 12. Simulated and measured reflection coefficient when the proposed antenna is operating in wideband state.

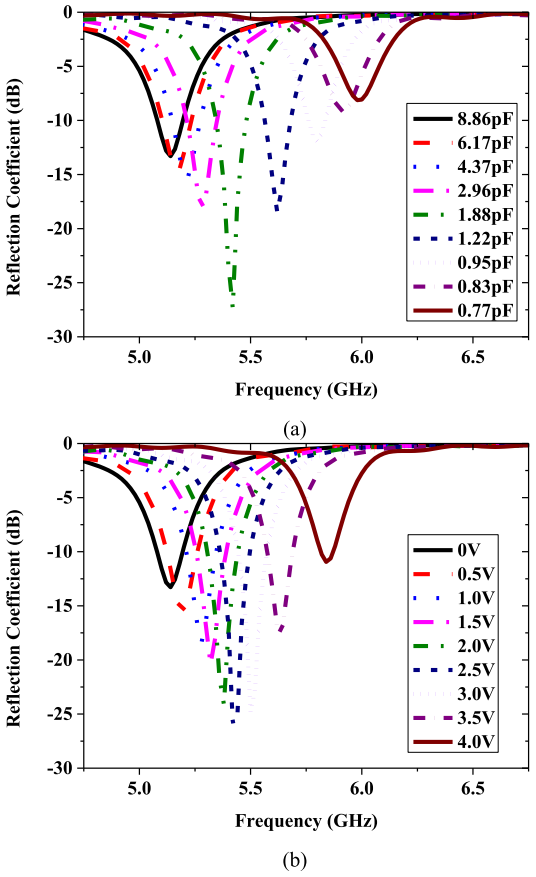

FIGURE 13. Simulated and measured reflection coefficient when the proposed antenna is operating in tunable narrowband state. (a) frequency(GHz). (b) frequency(GHz).

the proposed antenna is fabricated and measured. Fig. 11 demonstrates the photographs of the proposed DRA. In this paper, p-i-n diodes of SMP 1345-079LF produced by Skyworks for selecting the RF path for wideband state or tunable continuously narrowband state. Three dc biasing lines at the front of substrate and one at the ground plane are enough to actuating all the diodes. When connect to the microwave network analyzer for test, a dc-block SMA connector is required between the proposed DRA and the coaxial measurement cable. Agilent-N5227A vector network analyzer and the anechoic chamber with a dimension of $10 \times 6 \times 6$ m^3 were used for measuring the reflected coefficients, far-field radiation patterns and realized gains.

Fig. 12 shows the simulated and measured impedance performance for the proposed frequency-reconfigurable antenna at wideband state by activating p-i-n diode D1 only through dc biasing network. Good agreement between the measured and simulated results is obtained at the state with the impedance bandwidth of 5.12 GHz ranging from 3.82 GHz to 8.94 GHz.

The simulated and measured reflection coefficients for the tunable narrow band state by actuating p-i-n diodes D2 and D3 are demonstrated in Fig. 13(a) and (b). The measured tunable resonant frequency range is from 5.12 GHz to 5.86 GHz, while the simulated one is from 5.14 GHz to 5.98 GHz. The small frequency shift can be attributed for inaccuracies in fabrication, test and diode model data. In addition, compared to the reflection coefficients of the filter alone in Fig. 9, it can be seen that resonant performances change nonlinearly.

Fig. 14 depicts the simulated and measured far-field normalized radiation patterns at 4 GHz and 8 GHz in xoz-plane and yoz-plane, when the proposed frequency-reconfigurable DRA is operating at wideband state. The patterns in the xoz-plane with slight leans are the results of offset feed network, while the patterns in the yoz-plane reflect an approximately omnidirectional radiation characteristic. Reasonably good consistency can be found at both the principle planes, and the slight differences in the observed pattern results are mainly attributed to the fabrication tolerances, the antenna test positioning system and the external dc biasing wires coming from dc power supply. In addition, the realized gains ranging from 2.04 dBi to 4.69 dBi are obtained across the wideband operation bandwidth between 3.82 GHz to 8.94 GHz. The small deteriorated gain difference attributes to the same reason for the difference of reflected coefficients and radiation patterns as mentioned earlier.

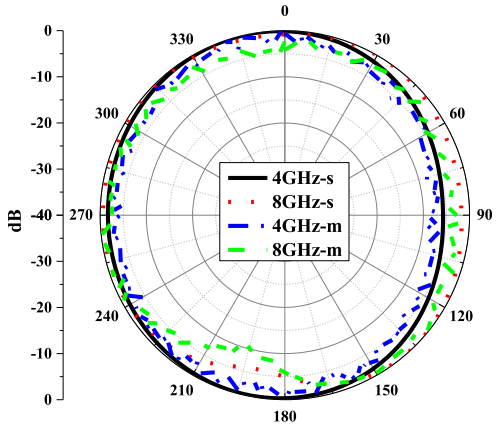

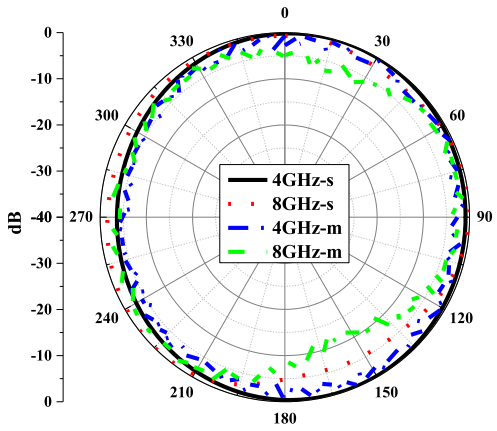

FIGURE 14. Simulated and measured normalized radiation patterns of the proposed DRA operated at wideband states in (a) xoz-plane and (b) yoz-plane.

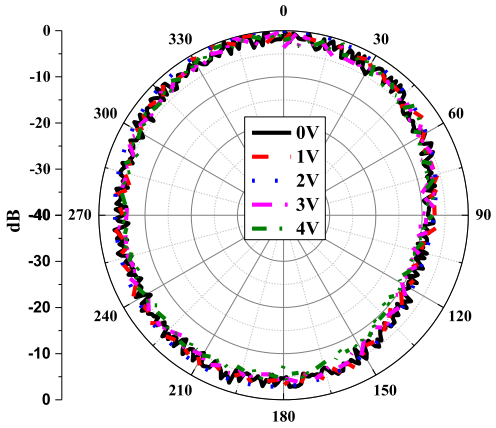

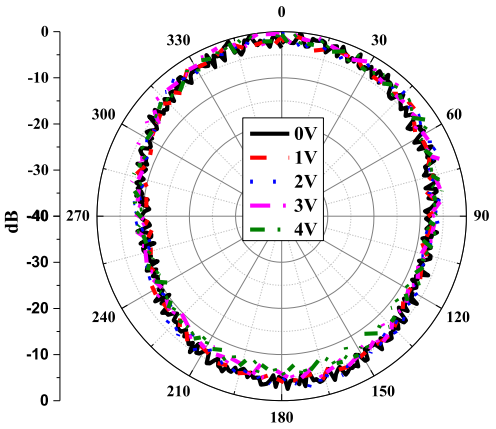

FIGURE 15. Measured normalized radiation patterns of the proposed DRA operated at tunable narrrowband states in (a) xoz-plane and (b) yoz-plane.

TABLE 4. Performance comparisons of wideband-to-narrowband tunable antennas.

Ref.	Wideband State Bandwidth (GHz)	Narrowband Tunable range (GHz)	Diode No.
[12]	2.2 GHz	3.9-4.82 GHz	3
[13]	2.63 GHz	3.05-4.39 GHz	3
[14]	2.72 GHz	0.57-0.68 GHz, 0.83-1.12 GHz	4
Our work	5.12 GHz	5.14-5.98 GHz	4

The measured normalized radiation patterns of the proposed DRA operated at tunable narrowband state in xoz-plane and yoz-plane is shown in Fig. 15. It can be observed that the patterns under different bias voltages are identical at its corresponding resonant frequencies 5.12 GHz (0V), 5.28 GHz (1V), 5.38GHz (2 V), 5.5 GHz (3 V) and 5.86 GHz (4 V), which depends on the unaltered antenna structure. The measured peak gains ranges from 3.73 dBi to 4.12 dBi across the tunable narrow bands by different bias voltages ranging from 0 V to 8 V.

Performance comparisons between the proposed DRA and other types of wideband-to-narrowband antennas with continuously tunable characteristics are indicated in Table 4, for no relevant DRAs reported. It is clear that, the technique for integrating with filter in the feedline by selecting RF path contributes to a broaden sensing wideband range, compared the method in [28] and [29], and it is more compact, no mutual coupling and easier fabrication in comparison with multiple ports for wideband-to-narrowband scheme in [30]. In addition, the proposed design gives new ideas for achieving frequency reconfigurable DRA.

IV. CONCLUSION

In this paper, a novel frequency-reconfigurable DRA with wideband and continuously tunable narrowband is proposed. The antenna is composed of a rectangular dielectric resonator excited by the microstrip feedline integrated with a reconfigurable bandpass filter. Two types of frequency reconfigurable states shift between through selecting relevant RF path by p-i-n diodes. Moreover, by tuning the reverse bias voltage of the varactor diode loaded in filter, the antenna is able to operate at a continuously tunable frequency band. Stable radiation patterns can be achieved at all operating frequencies. To demonstrate its functionality effectively, a prototype with

wideband of 5.12 GHz and tunable operating frequency from 5.14 GHz to 5.98 GHz was fabricated, measured and verified with a good consistency for the proposed design. The antenna is suitable for cognitive radio system incorporating UWB and WLAN systems. To further develop this work, some promising reconfigurable filters, which can be integrated with feed network for DRA and provide broaden tunable frequency ranges, and UWB DRA will be proposed and adopted to future wireless communications.

REFERENCES

[1] S. Haykin, "Cognitive radio: Brain-empowered wireless communications," *IEEE J. Sel. Areas Commun.*, vol. 23, no. 2, pp. 201–220, Feb. 2005.

[2] J. Motola, "Cognitive radio architecture evolution," *Proc. IEEE*, vol. 97, no. 4, pp. 626–641, Apr. 2009.

[3] J. T. Bernhard, *Reconfigurable Antennas*. London, U.K.: Morgan & Claypool, 2007.

[4] J. Costantine, Y. Tawk, S. E. Barbin, and C. G. Christodoulou, "Reconfigurable antennas: Design and applications," *Proc. IEEE*, vol. 103, no. 3, pp. 424–437, Mar. 2015.

[5] L. Ge and K. M. Luk, "Frequency-reconfigurable low-profile circular monopolar patch antenna," *IEEE Trans. Antennas Propag.*, vol. 62, no. 7, pp. 3443–3449, Jul. 2014.

[6] K. Yoshitomi, H. A. Atallah, A. B. Abdel-Rahman, K. Yoshitomi, and R. K. Pokharel, "Compact frequency reconfigurable filtennas using varactor loaded T-shaped and H-shaped resonators for cognitive radio applications," *IET Microw., Antennas Propag.*, vol. 5, no. 8, pp. 991–1001, 2016.

[7] Y.-M. Cai, K. Li, Y. Yin, S. Gao, W. Hu, and L. Zhao, "A low-profile frequency reconfigurable grid-slotted patch antenna," *IEEE Access*, vol. 6, pp. 36305–36312, 2018.

[8] T. Aboufoul, A. Alomainy, and C. Parini, "Reconfiguring UWB monopole antenna for cognitive radio applications using GaAs FET switches," *IEEE Antennas Wireless Propag. Lett.*, vol. 11, pp. 392–394, 2012.

[9] A. Mansoul, F. Ghanem, M. R. Hamid, and M. Trabelsi, "A selective frequency-reconfigurable antenna for cognitive radio applications," *IEEE Antennas Wireless Propag. Lett.*, vol. 13, pp. 515–518, 2014.

[10] G. Srivastava, A. Mohan, and A. Chakrabarty, "Compact reconfigurable UWB slot antenna for cognitive radio applications," *IEEE Antennas Wireless Propag. Lett.*, vol. 16, pp. 1139–1142, 2017.

[11] J. Deng, S. Hou, L. Zhao, and L. Guo, "Wideband-to-narrowband tunable monopole antenna with integrated bandpass filters for UWB/WLAN applications," *IEEE Antennas Wireless Propag. Lett.*, vol. 16, pp. 2734–2737, 2017.

[12] P. Y. Qin, F. Wei, and Y. J. Guo, "A wideband-to-narrowband tunable antenna using a reconfigurable filter," *IEEE Trans. Antennas Propag.*, vol. 63, no. 5, pp. 2282–2285, May 2015.

[13] M.-C. Tang, Z. Wen, H. Wang, M. Li, and R. W. Ziolkowski, "Compact, frequency-reconfigurable filtenna with sharply defined wideband and continuously tunable narrowband states," *IEEE Trans. Antennas Propag.*, vol. 65, no. 10, pp. 5026–5034, Oct. 2017.

[14] R. Hussain and M. S. Sharawi, "A cognitive radio reconfigurable MIMO and sensing antenna system," *IEEE Antennas Wireless Propag. Lett.*, vol. 14, pp. 257–260, 2015.

[15] K. R. Jha, B. Bukhari, C. Singh, G. Mishra, and S. K. Sharma, "Compact planar multistandard MIMO antenna for IoT applications," *IEEE Trans. Antennas Propag.*, vol. 66, no. 7, pp. 3327–3336, Jul. 2018.

[16] A. Petosa, *Dielectric Resonator Antenna Handbook*. Norwood, MA, USA: Artech House, 2007.

[17] A. Petosa and A. Ittipiboon, "Dielectric resonator antennas: A historical review and the current state of the art," *IEEE Antennas Propag. Mag.*, vol. 52, no. 5, pp. 91–116, Oct. 2010.

[18] G. H. Huff, D. L. Rolando, P. Walters, and J. McDonald, "A frequency reconfigurable dielectric resonator antenna using colloidal dispersions," *IEEE Antennas Wireless Propag. Lett.*, vol. 9, pp. 288–290, 2010.

[19] C. X. Hao, B. Li, K. W. Leung, and X. Q. Sheng, "Frequency-tunable differentially fed rectangular dielectric resonator antennas," *IEEE Antennas Wireless Propag. Lett.*, vol. 10, pp. 884–887, 2011.

[20] J. Desjardins, D. A. McNamara, S. Thirakoune, and A. Petosa, "Electronically frequency-reconfigurable rectangular dielectric resonator antennas," *IEEE Trans. Antennas Propag.*, vol. 60, no. 6, pp. 2997–3002, Jun. 2012.

[21] J.-B. Yan and J. T. Bernhard, "Implementation of a frequency-agile MIMO dielectric resonator antenna," *IEEE Trans. Antennas Propag.*, vol. 61, no. 7, pp. 3434–3441, Jul. 2013.

[22] Y. F. Wang, N. Z. Wang, T. A. Denidni, Q. S. Zeng, and G. Wei, "Integrated ultrawideband/narrowband rectangular dielectric resonator antenna for cognitive radio," *IEEE Antennas Wireless Propag. Lett.*, vol. 13, pp. 694–697, 2014.

[23] T. Apperley and M. Okoniewski, "An air-gap-based frequency switching method for the dielectric resonator antenna," *IEEE Antennas Wireless Propag. Lett.*, vol. 13, pp. 455–458, 2014.

[24] S. Danesh, S. K. A. Rahim, M. Abedian, and M. R. Hamid, "A compact frequency-reconfigurable dielectric resonator antenna for LTE/WWAN and WLAN applications," *IEEE Antennas Wireless Propag. Lett.*, vol. 14, pp. 486–489, 2015.

[25] S. Danesh, M. R. Kamarudin, T. A. Rahman, M. Abedian, M. H. Jamaluddin, and M. Khalily, "A C-shaped dielectric resonator antenna with frequency reconfigurable for ISM and LTE band applications," *Microw. Opt. Technol. Lett.*, vol. 59, no. 3, pp. 134–138, Jun. 2016.

[26] S. Pahadsingh and S. Sahu, "Planar UWB integrated with multi narrowband cylindrical dielectric resonator antenna for cognitive radio application," *AEU—Int. J. Electron. Commn.*, vol. 74, pp. 150–157, Apr. 2017.

[27] R. D. Gupta and M. S. Parihar, "Dual/wideband hybrid DRA with reconfigurable operation," *Int. J. Microw. Wireless Technol.*, vol. 9, no. 2, pp. 387–394, 2017.

[28] Y. Hao, Q. Wang, X. Gao, S. Huang, and K. Bi, "Frequency tunable slot-coupled dielectric resonators antenna," *J. Alloys Compounds*, vol. 702, pp. 664–668, Apr. 2017.

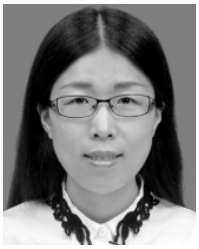

BEI-JIA LIU was born in Heilongjiang, China, in 1988. She received the B.S. degree in communication engineering from the Harbin University of Science and Technology, Harbin, China, in 2010, and the M.S. degree in information and communication engineering from the Harbin Institute of Technology, in 2013, where she is currently pursuing the Ph.D. degree in electromagnetic field and microwave technology.

She joined the Harbin Institute of Technology, as an Assistant Engineer, in 2013, was promoted to an Engineer, in 2016. Her research interests include dielectric resonator antenna and reconfigurable antenna.

JING-HUI QIU was born in Heilongjiang, China, in 1960. He received the B.S. degree in radio engineering, the M.S. degree in communication and information systems, and the Ph.D. degree in communication and information systems from the Harbin Institute of Technology, in 1982, 1987, and 2008.

From 1982 to 1987, he was a Teaching Assistant with the Harbin Institute of Technology. From 1987 to 1992, he promoted as a Lecturer, and then became an Associate Professor. He was promoted as a Professor, in 2002. He has authored and co-authored over 100 publications (book chapters, journal papers, and conference articles). His research interests include in the field of electromagnetic theory, microwave devices, antennas and millimeter-wave imaging.

SHENG-CHANG LAN was born Liaoning, China, in 1981. He received the B.S. degree in electronic engineering and the Ph.D. degree in information and communication engineering from the Harbin Institute of Technology, in 2005 and 2011, respectively.

From 2008 to 2014, he was with the Research Center of Satellite Technology, Harbin Institute of Technology. From 2012 to 2013, he did Postdoctoral Research with the Department of Radio Science and Engineering, Aalto University. Since 2014, he has been an Associate Professor with the Department of Microwave Engineering, Harbin Institute of Technology. He has authored over 40 articles, and over 20 inventions. His research interests include automobile radar signal processing, UWB antenna, and deep learning in the microwave fields for sensing and medical applications.

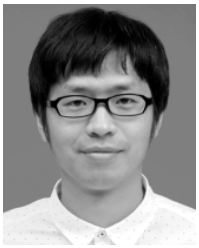

GUO-QIANG LI was born in Heilongjiang, China, in 1985. He received the B.S. degree in information and computing science from Northeast Agriculture University, Harbin, China, in 2008, and the M.S. degree in applied mathematics from Harbin Engineering University, Harbin, in 2011.

From 2011 to 2014, he was with Zhongxing Telecommunication Equipment Corporation. He has been with Harbin Kejia General Mechanical and Electrical Company, Harbin, as an Engineer, since 2014. His research interests include information fusion image recognition algorithm, millimeter-wave imaging, and electromagnetic field theory.